Interactions in Large, Polyaromatic Hydrocarbon Dimers: Application of Density Functional Theory with Dispersion Corrections

Iain D. Mackie and Gino A. DiLabio*

National Institute for Nanotechnology, National Research Council of Canada, 11421 Saskatchewan Drive, Edmonton, Alberta, Canada T6G 2M9

Received: July 12, 2008; Revised Manuscript Received: August 13, 2008

The interactions within two models for graphene, coronene and hexabenzocoronene (HBC), and $(H_3C(CH_2)_5)_6$-HBC, a synthesizable model for asphaltenes, were studied using density functional theory (DFT) with dispersion corrections. The corrections were implemented using carbon atom-centered effective core-type potentials that were designed to correct the erroneous long-range behavior of several DFT methods. The potentials can be used with any computational chemistry program package that can handle standard effective core potential input, without the need for software modification. Testing on a set of common noncovalently bonded dimers shows that the potentials improve calculated binding energies by factors of 2−3 over those obtained without the potentials. Binding energies are predicted to within ca. 15%, and monomer separations to within ca. 0.1 Å, of high-level wave function data. The application of the present approach predicts binding energies and structures of the coronene dimer that are in excellent agreement with the results of other DFT methods in which dispersion is taken into account. Dimers of HBC show extensive binding in π-stacking arrangements, with the largest binding energy, 44.8 kcal/mol, obtained for a parallel-displaced structure. This structure is inline with the published crystal structure. Conformations in which the monomers are perpendicular to one another are much more weakly bound and have binding energies less than 10 kcal/mol. For dimers of $(H_3C(CH_2)_5)_6$-HBC, which contain 336 atoms, we find that a slipped-parallel structure with C_s symmetry has a binding energy of 52.4 kcal/mol, 8.9 kcal/mol lower than that of a bowl-like, C_{6v}-symmetric structure.

1. Introduction

Polyaromatic structures have great importance in many fields of physics and chemistry. For example, research involving graphene[1] and smaller polycyclic aromatics such as pentacene[2] has become increasingly significant in the area of molecular electronics applications. Additional interest in large, planar aromatic systems stems from their function as common components of asphaltenes,[3,4] which are heavy fractions of bitumen and heavy oil. The tendency of planar aromatic systems to strongly self-associate leads to interesting electronic properties in graphene multilayers,[5] but the same tendency in asphaltenes is problematic for a variety of processes related to the petroleum industry, including extraction and upgrading. Understanding the interactions between large, polyaromatic molecules is therefore of general importance in varied areas of physical chemistry.

Quantum mechanical studies of large, planar aromatic systems can, in principle, provide valuable insights into the chemical and electronic properties of these dispersion-bound systems. Because of their large size, density functional theory (DFT) methods are the only ones that can practically treat these systems, which can exceed several hundred atoms. However, there is a distinct lack of common density functionals to accurately describe dispersion interactions. Indeed, even correlated wave function methods have known deficiencies in this area.[6] Given the importance of dispersion to the nuclear structure of and electronic coupling between noncovalently bound systems such as polyaromatic dimers, this problem is not a trivial one.

There have been numerous published attempts to treat dispersion more accurately within the confines of DFT. Many of these have been recently reviewed by Sato et al.[7] Not included in ref 7 is the work of Rothlisberger and co-workers and their library of dispersion-corrected potentials for use in periodic DFT calculations.[8] Dispersion corrections of the form C_6/R^6 to the DFT energy have been successfully implemented by Grimme's group with empirical C_6 coefficients[9] and by Johnson and Becke using nonempirical coefficients based on exchange dipole moments.[10]

There has also been considerable activity in the development of new functionals that are able to treat van der Waals interaction phenomena. For example, efforts by Zhao and Truhlar,[11] Langreth and co-workers,[12] Hirao and co-workers,[13] and Head-Gordon et al.[14] have all met with certain success.

More recently, we described a simple method for correcting the erroneous long-range behavior of some DFTs by using carbon atom-centered effective core-type potentials (ECPs).[15] Our approach was based on one that we used to develop atom-centered quantum capping potentials[16] to deal with the link-atom problem in quantum mechanic/molecular mechanics modeling[17] and for calculating vibrations in truncated systems.[18] It was shown that the inclusion of carbon-centered ECPs with certain standard density functionals can result in remarkable improvement to binding energies (BEs) for noncovalently bound dimer systems.[15] It is important to highlight here the benefits of such an approach: This method involves only minor modification to standard input files of the type required for common computational chemistry programs, for example, Gaussian[19] and Molpro,[20] without the need to alter software code, thus making it easy to implement and use. Its use in such computational packages means that minimum-energy and transition-state geometries are optimized, frequencies calculated, and

* To whom correspondence should be addressed. Phone: (780) 641-1729. E-mail: Gino.DiLabio@nrc.ca.

10.1021/jp806162t CCC: $40.75
Published on Web 10/02/2008

molecular properties extracted in the usual manner and with only a minor increase in computing time. As will be shown, BEs determined using relatively small basis sets become comparable to those determined by other methods with large basis sets.

Reference 15 describes our prelimary exploration of the use of carbon-centered ECPs for use with PBE,[21] PW91,[22] and B971[23] density functionals. The goal of the present work is two-fold. First, we expand on our original work by developing optimized carbon-centered ECPs for a larger number and variety of density functionals and for basis sets of various sizes. The ECPs are tested on a large number of noncovalently bound dimers and on a series of reactions in which dispersion interactions are believed to be important. We then apply our method to polyaromatic hydrocarbon dimer systems that serve as model systems for molecular electronics and/or asphaltene chemistry.

2. Carbon Potential Optimization and Benchmarking

2.1. Carbon Atom-Centered Effective Potentials. The details of the development behind the ECP approach can be found in ref 15. To summarize, the method involves the addition of Gaussian-type functions to atom-centered effective core potentials such as that described:

$$U_l(r) = r^{-2}\sum_{i=1} c_{li} r^{n_{li}} e^{-\zeta_{li} r^2} \quad (1)$$

Potentials can be chosen to modify any element, but the poor treatment of dispersion in DFT is a problem that mostly affects group 4 and noble gas atoms, so we limit ourselves here to deal with carbon atoms and their application to carbon-containing, noncovalently bound dimers. From herein such potentials are referred to as C-Pots. Two Gaussians are used—one to reproduce weakly attractive medium- to long-range character, ζ_1, and the second a tighter, repulsive potential to prevent overbinding, ζ_2. ζ_1 was chosen to be 0.08 and ζ_2 = 0.12,[15] values that are small enough so that the C-Pots do not significantly perturb the geometries and electronic structure of monomers from that obtained without the potentials. These values for ζ were subsequently kept fixed during the course of the succeeding calculations.

For this work the Gaussian 03 suite of programs[19] was used for all calculations. None of the energies reported were corrected for zero-point vibration. The potentials are incorporated into a standard input file as a high angular momentum function (L = 3) with single s, p, and d potential functions set to zero. For a sample input the reader is directed to the Supporting Information (SI).

Values for the coefficients, c_{li}, were systematically adjusted to minimize the percent absolute deviation (AD, %) between calculated BEs and literature values for a set of noncovalently bound dimers. c_1 and c_2 were optimized for a mix of hybrid and pure functionals, chosen on the basis of their abilities to treat different problems common in computational chemistry or for their general popularity: B971,[23] PBE,[21] PBE1,[24] PW91,[22] B3[25]LYP,[26] and BHandH[27]LYP.[26] Basis sets spanning a large range in sizes were used with each functional: 6-31G(d,p), 6-31+G(d,p), 6-311+G(2d,2p), and aug-cc-pVTZ. Optimized coefficient values are recorded in Table 1 for the set of dimers, originally used in ref 15, listed in Table 2. Data obtained using 6-31G(d,p) basis sets were generally inferior to those obtained using larger basis sets and are presented in Table S1 of the SI. Data with the PW91 and BHandHLYP functionals are generally similar to those obtained using the PBE and B3LYP functionals, respectively, so the former data sets are also relegated to the SI; see Table S1.

TABLE 1: Summary of Optimized Coefficients[a] c_1[b] and c_2[c] Established for the Set of Noncovalently Bound Dimers As Found in Table 2

	B971 method	PBE method	PBE1 method	B3LYP method
6-31+G(d,p) Basis Set				
c_1	−0.001438	−0.001550	−0.001559	−0.001520
c_2	+0.003475	+0.003300	+0.003500	+0.001300
AD(HC) (%)	7.5	12.6	11.4	33.6
AD(hetero) (%)	21.3	23.9	18.3	11.0
AD[d] (%)	13.8	17.7	14.5	23.3
6-311+G(2d,2p) Basis Set				
c_1	−0.001534	−0.001687	−0.001669	−0.001600
c_2	+0.003654	+0.003735	+0.003735	+0.001280
AD(HC) (%)	8.7	11.5	13.4	37.1
AD(hetero) (%)	12.9	21.6	17.2	15.7
AD[e] (%)	10.5	16.1	15.1	27.4
aug-cc-pVTZ Basis Set				
c_1	−0.001534	−0.001687	−0.001687	−0.001600
c_2	+0.003580	+0.003511	+0.003511	+0.001280
AD(HC) (%)	9.4	11.3	13.0	35.1
AD(hetero) (%)	10.5	12.0	7.2	13.6
AD[f] (%)	9.9	11.6	10.4	25.3

[a] The coefficients of the C-Pots are optimized for use with the indicated DFT methods. Shown are the percent absolute deviations of the binding energies for the hydrocarbon dimers (AD(HC), %) and the heterodimers (AD(hetero), %) and the total percent absolute deviations for the entire set of dimers (AD, %). The set of dimers is listed in Table 2. For the purposes of AD (%) evaluations, metastable species were assigned errors of 100%. [b] ζ_1 = 0.08. [c] ζ_2 = 0.12. [d] With no C-Pot, AD (%) (AD(HC) (%)/AD(hetero) (%)): B971, 35.3 (49.8/17.9); PBE, 43.4 (58.6/25.1); PBE1, 45.1 (64.7/21.6); B3LYP, 70.5 (91.2/45.5). [e] With no C-Pot, AD (%) (AD(HC) (%)/AD(hetero) (%)): B971, 38.6 (59.7/13.3); PBE, 46.6 (69.4/19.2); PBE1, 46.7 (72.4/15.8); B3LYP, 68.2 (94.6/36.5). [f] With no C-Pot, AD (%) (AD(HC) (%)/AD(hetero) (%)): B971, 42.0 (61.3/18.7); PBE, 50.0 (69.7/26.3); PBE1, 52.4 (73.8/26.7); B3LYP, 72.2 (95.0/44.7).

It is very important to point out that the BEs that are calculated in the course of optimizing the coefficients of the C-Pots are not corrected for basis set incompleteness. Therefore, the C-Pots tend to compensate for basis set superposition error (BSSE), and it is therefore worth warning against the use of corrections such as counterpoise[28] with our approach for correcting some of the long-range problems in DFT.

The set of noncovalently bound dimers used to generate the optimized C-Pots encompass a mixture of hydrocarbons and molecules containing heteroatoms such as O, N, and F, in addition to C atoms. Included are the benzene dimers: parallel (P), slipped parallel (SP), and T-shaped (T). Also incorporated into the set are the naphthalene dimers: T-shaped (T), T-shaped cross (TC), parallel (P), and parallel crossed (PC). These structures of the naphthalene dimers can be seen in Figure 1 of ref 29. The TC isomer is configured such that one naphthalene is rotated in its molecular plane by 90°, while the P configuration has also been described in the literature as "stacked". The use of dimers of molecules containing heteroatoms, from hereon referred to as heterodimers, allows scrutiny of the applicability of the method to systems where not only is dispersion important but also dipole−dipole, dipole−induced dipole, and/or hydrogen-bonding interactions. For brevity Table 2 is arranged into two sections—one detailing the binding energies for the hydrocarbons

TABLE 2: Binding Energies (kcal/mol) for the Set of Noncovalently Bound Dimers Using Method/6-31+G(d,p) with Optimized Carbon Potentials

	B971	PBE	PBE1	B3LYP	high-level result[a]
Hydrocarbons					
$CH_4 \cdot C_6H_6$	1.26	1.16	1.15	0.70	1.23[b]
$(CH_4)_2$	0.44	0.33	0.28	*−0.02*[c]	0.51[d]
$CH_4 \cdot C_2H_4$	0.58	0.54	0.46	0.18	0.50[e]
P-$(C_6H_6)_2$	1.50	1.57	1.36	1.06	1.70[f]
SP-$(C_6H_6)_2$	2.49	2.68	2.60	2.63	2.61[f]
T-$(C_6H_6)_2$	2.40	2.36	2.37	1.91	2.62[f]
$(C_2H_4)_2$	1.38	1.25	1.20	0.75	1.42[d]
$(C_2H_2)_2$	1.59	1.53	1.45	1.19	1.34[d]
P-$(C_{10}H_8)_2$	3.73	2.50	3.76	3.82	3.78[g]
PC-$(C_{10}H_8)_2$	5.22	5.83	5.81	6.45	5.28[g]
T-$(C_{10}H_8)_2$	4.14	4.08	4.16	3.45	4.34[g]
TC-$(C_{10}H_8)_2$	2.96	2.92	2.84	2.21	3.09[g]
MAD	0.12	0.28	0.19	0.55	
AD (%)	7.5	12.6	11.4	33.6	
Heteroatoms					
$HCN \cdot HF$	8.07	8.51	8.23	8.01	7.30[e]
$C_2H_4 \cdot HF$	5.70	6.38	5.86	5.82	4.47[h]
$(CF_4)_2$	1.06	1.04	1.00	0.70	0.78[i]
$(CH_3F)_2$	2.85	2.77	2.67	2.66	2.33[h]
$CH_4 \cdot HF$	1.72	1.98	1.71	1.47	1.65[e]
$CH_4 \cdot NH_3$	1.19	1.24	1.10	0.71	0.73[e]
$(CO_2)_2$	1.47	1.33	1.41	1.51	1.34[j]
$(H_2CO)_2$	3.96	3.62	3.87	3.68	3.37[e]
$H_2O \cdot C_6H_6$	3.75	3.77	3.74	3.20	3.17[k]
$(H_3CCN)_2$	5.81	5.65	5.76	5.57	6.16[h]
MAD	0.50	0.61	0.48	0.38	
AD (%)	21.3	23.9	18.3	11.0	
MAD (total)	0.29	0.43	0.32	0.47	
AD (%) (total)	13.8	17.7	14.5	23.3	

[a] The high-level data are generally of large basis set, CCSD(T) quality, with the exception of those for the naphthalene dimers; see ref 29 For full details, see the respective reference. [b] Reference 31. [c] Metastable complex. [d] Reference 32. [e] Reference 10a. [f] Reference 33. [g] Reference 29. [h] Reference 6. [i] Reference 34. [j] Reference 35. [k] Reference 36.

TABLE 3: Deviations in Monomer Separations (Å), Relative to High-Level Theoretical Results, for the Set of Noncovalently Bound Dimers Using Method/6-31+G(d,p) with Optimized Carbon Potentials

	separation[a]	B971	PBE	PBE1	B3LYP	high-level result[b]
Hydrocarbons						
$CH_4 \cdot C_6H_6$	$H_4C-CM(C_6H_6)$	0.1	0.1	0	0.1	3.8
$(CH_4)_2$	C−C	0.1	0.3	0.2	0.3	3.6
$CH_4 \cdot C_2H_4$	$H_4C-CM(C_2H_4)$	0	0	0	0.1	4.2
P-$(C_6H_6)_2$	CM−CM	0	−0.1	−0.1	−0.1	3.9
SP-$(C_6H_6)_2$	CM−CM	0.1	−0.1	−0.1	−0.2	3.9
T-$(C_6H_6)_2$	CM−CM	0.1	0.1	0	0	5.0
$(C_2H_4)_2$	CM−CM	0	0	0	−0.1	3.8
$(C_2H_2)_2$	CM−CM	0	0	0	0	4.2
P-$(C_{10}H_8)_2$	CM−CM	0	−0.1	−0.1	−0.2	3.8
PC-$(C_{10}H_8)_2$	CM−CM	0	−0.1	−0.2	−0.3	3.6
T-$(C_{10}H_8)_2$	CM−CM	0.1	0.1	0.1	0	5.0
TC-$(C_{10}H_8)_2$	CM−CM	0.1	0.1	0	0	5.2
MAD		0.05	0.08	0.07	0.12	
Heteroatoms						
$HCN \cdot HF$	N−HF	−0.1	−0.1	−0.1	−0.1	1.9
$C_2H_4 \cdot HF$	$FH-CM(C_2H_4)$	0	0.1	−0.1	−0.1	2.2
$(CF_4)_2$	C−C	0	0.1	0	0	4.0
$(CH_3F)_2$	C−C	−0.1	−0.1	−0.1	−0.1	3.9
$CH_4 \cdot HF$	C−HF	0.1	0	0	0	2.3
$CH_4 \cdot NH_3$	C−N	−0.2	−0.2	−0.2	−0.2	3.9
$(CO_2)_2$	C−C	0.1	0.1	0.1	−0.1	3.6
$(H_2CO)_2$	C−C	0	0	0	0	3.6
$H_2O \cdot C_6H_6$	$O-CM(C_6H_6)$	0	0	−0.1	−0.1	3.4
$(H_3CCN)_2$	C−C	0	−0.1	−0.1	−0.1	3.4
MAD		0.06	0.08	0.08	0.08	
MAD (total)		0.05	0.08	0.07	0.10	

[a] CM = center-of-mass of heavy atoms. [b] The high-level data, taken mostly from ref 6, are generally of large basis set, CCSD(T) quality, with the exception of those of naphthalene dimers; see ref 29.

and another showing the heterodimer data. Binding energies are defined as the difference in energy between the dimer and two separate monomers. C-Pots are applied to both the dimer and corresponding monomers to determine BEs. Neither zero-point energies nor vibration corrections to the enthalpy are included in these data.

Table 1 shows the optimized coefficients for C-Pots and the subsequent method and basis set dependence on the AD (%) for the set of dimers. The values of c_1 tend to be smaller in magnitude when smaller basis sets are used; see also Table S1 in the SI. This is because basis set incompleteness plays a more important role in apparent dispersion binding with smaller basis sets, so there is a lesser need for dispersion-correcting potentials. For a given basis set, the B86-based functionals (B971, PBE, PBE1, and PW91) all have quite similar coefficients, implying that these functionals have comparable long-range behavior, which is consistent with literature reports.[30] This finding also implies that the C-Pots are *very nearly* transferrable between related DFT methods. Not surprisingly,[30,6] the B86-based functionals easily outperform the B88-based B3LYP (and BHandHLYP; see the SI) functionals. For example, with the aug-cc-pVTZ basis set, C-Pot-corrected B971 manages an AD as low as 9.9%, while in comparison B3LYP is capable of 25.3%. These results are consistent with the ADs obtained using aug-cc-pVTZ basis sets with uncorrected DFTs, viz., 42.0% for B971 and 72.2% for B3LYP. Because the B88-based functionals tend to be more repulsive than the B86-based functionals, the C-Pot coefficients for the former are such that they result in an overall larger attractive correction to the intermononer potential.

With all DFTs, little improvement in AD (%) is found in increasing the basis set size from 6-31+G(d,p) to 6-311+G(2d, 2p). In these cases, the heterodimer subsets have larger AD (%) values than the hydrocarbon subsets. This reflects the fact that the heterodimers tend to be overbound as a result of basis set incompleteness, a problem that is slightly compounded by the use of C-Pots, viz., AD(hetero) (B971/6-31G(d,p)−C-Pots) = 21.3% vs AD(HC) (B971/6-31G(d,p)) = 17.9%. This overbinding is alleviated upon increasing the basis set size to aug-cc-pVTZ, and the AD (%) values for the heterodimer sets become more in line with those of the hydrocarbon set. This finding is in agreement with our expectations that DFT methods generally perform better for stronger noncovalent interactions, such as hydrogen bonds, than they do for weaker ones, such as dispersion interactions; see Figure 2 of ref 6.

In general, the data in Table 1 show that the simple carbon-centered C-Pots are capable of greatly correcting much of the deficient long-range behavior in all of the DFT methods tested. The AD (%) values indicate that the C-Pots provide factors of 2−3 improvement in BEs relative to the values obtained when C-Pots are not used.

The explicit BEs computed for each of the dimers in the set of dimers used to optimize the C-Pot coefficients are given in

TABLE 4: Binding Energies (kcal/mol) Calculated by PBE1/6-31+G(d,p) with Optimized Carbon Potentials for a Portion of the S22 Set[37] (AD (%) in Parentheses)

	PBE1/6-31+ G(d,p)-C-Pots	PBE1/6-31+ G(d,p)	reference data[a]
Hydrogen-Bonded Complexes			
$(HCOOH)_2$	18.11 (2.7)	17.45 (6.2)	18.61
$(HCONH_2)_2$	15.45 (3.2)	14.90 (6.6)	15.96
uracil dimer (C_{2h})	19.61 (5.0)	18.82 (8.9)	20.65
2-$C_8H_{11}NO_3$·2-$(C_5H_6N_2)_2$	16.28 (2.6)	15.47 (7.4)	16.71
adenine·thymine WC	15.70 (4.1)	14.62 (10.7)	16.37
AD (%)	3.5	8.0	
Dispersion-Dominated Complexes			
$(C_4H_4N_2)_2$	3.77 (14.7)	1.23 (72.1)	4.42
uracil dimer (C_2)	8.31 (17.9)	[b,c]	10.12
C_8H_7N·C_6H_6 (C_1)	4.54 (13.0)	[c,d]	5.22
adenine·thymine stack	9.91 (19.0)	4.47 (63.4)	12.23
AD (%)	16.2	67.8[e]	
Mixed Complexes			
C_2H_4·C_2H_2	1.66 (8.5)	1.43 (6.4)	1.53
NH_3·C_6H_6	2.13 (9.4)	1.59 (32.2)	2.35
HCN·C_6H_6	4.81 (7.9)	3.68 (17.6)	4.46
T-C_8H_7N•C_6H_6	4.92 (14.1)	3.41 (40.5)	5.73
$(C_6H_5OH)_2$	7.24 (2.7)	6.02 (14.6)	7.05
AD (%)	8.5	22.6	
AD (%) (total)	8.9		

[a] The reference data are generally of CCSD(T)/complete basis set quality. [b] Not stable. Optimizes to the hydrogen-bonded structure. [c] AD (%) is undefined. [d] Not stable. Optimizes to the T-structure. [e] Average for the two bound structures.

Table 2. We judge the 6-31+G(d,p) basis set to give the best balance of computing time and quality of the results. For this reason we limit the data in Table 2 to include only the 6-31+G(d,p) results, with the remainder relegated to the SI. From Table 2, we see that B971, PBE, and PBE1 show similar abilities to replicate high-level BEs for the set of dimers, with B971 having the slight edge over PBE1 for the hydrocarbons and overall. However, the PBE1 method is better for the heterodimers. As described above, most methods are better equipped at dealing with hydrocarbons over heterodimers, with the exceptions being B3LYP and BHandHLYP (see the SI for the latter data). While both B971 and PW91 have AD values of less than 8% for the hydrocarbon subset, PW91 is disappointingly poor for the heterodimers, with an AD of 36.7% for this subset; see Tables S1 and S2 in the SI. B971 in contrast gives a good AD of 21.3% for the heterodimers.

BE calculations carried out by Johnson and Becke on the same set of dimers, in their efforts to develop new functionals to deal with van der Waals forces, gave an AD of 17.5%.[10b] Compare this to the best and worst values of 13.8% (B971) and 23.5% (B3LYP) determined here using the 6-31+G(d,p) basis set with optimized C-Pots. The DF07 functional developed and employed by Johnson and Becke is able to treat the hydrocarbon and heterodimer subsets nearly equivalently, with AD values of 19.5% and 15.1%, respectively.

The inability of MP2 to replicate high-level BEs for van der Waals complexes can also be reaffirmed.[6,37] For the hydrocarbon subset used here, MP2 counterpoise-corrected and basis-set-extrapolated energies give an AD of 51.1%, while the heterodimers muster 25.7%, resulting in a mean AD of 39.6%, thus adding further weight to the comment made by Jureĕka et al. that "MP2...is insufficient and whenever significant dispersion contribution is expected a correction for higher order correlation effects must be applied." [37] The spin-scaled variant of MP2 (SCS-MP2) has made headway in this regard.[38]

The monomer separations in the dimers listed in Table 2 are presented in Table 3 using method/6-31+G(d,p) with optimized C-Pots (see Table 1). The monomer separations are generally in very good agreement with available high-level data. The largest deviations are obtained using B3LYP on the methane dimer (0.3 Å too long) and the "PC" naphthalene dimer (0.3 Å too short). The majority of the structures have monomer separations with a deviation relative to the high-level data of up to 0.1 Å. It should be pointed out that the potential energy surfaces associated with most noncovalent interactions are very flat, so 0.1−0.2 Å changes in the monomer separations result in only small differences in the BEs.

The data in Table 3 show that C-Pots can be used to predict, at low computational cost, fairly accurate monomer separations in noncovalently bonded systems. This has particular significance in modeling of large structures, viz., interacting polyaromatic systems, as is done in the present work (vide infra) or problems such as protein structure modeling, in which noncovalent interactions play an important role in protein folding.

2.2. Testing of Carbon Potentials. ***2.2.1. Other Noncovalently Bound Dimers.*** The PBE1/6-31+G(d,p) approach with optimized C-Pots strikes a good balance between computational speed and accuracy in BE prediction, for both hydrocarbon and heterodimer systems; see Tables 1 and 2. We chose to further examine the applicability of this approach on a set of noncovalently bonded dimers not used in the optimization of the C-Pots. The so-called S22 set, devised by Jureĕka et al.,[37] is a collection of large-basis-set, ΔCCSD(T)-corrected interaction energies for a series of weakly bonded complexes. This set has become the benchmark to which new DFT functionals and methodologies are compared. The S22 set is made up of three classes of complexes: (a) hydrogen-bonded complexes, (b) those in which dispersion forces dominate, and (c) those which contain a mix of electrostatic and dispersion contributions. For comparative purposes, we computed the binding energies for carbon-containing dimers[39] from all three classes, excluding those that were used in the optimization of the C-Pots. The reader is directed toward Table S4 in the SI for BEs for the full S22 set calculated using our method, with comparisons to BEs determined by recently developed functionals, designed with van der Waals complexes particularly in mind.[40,41] The structures of the dimers comprising the S22 set are shown in ref 37.

The PBE1/6-31+G(d,p) method with the optimized C-Pot method gives an excellent mean AD value of 3.5% for the hydrogen-bonded dimers. This represents a minor improvement over the BEs obtained without the use of C-Pots, viz., AD = 8.0%, and reflects the fact that DFTs tend to do reasonably well for hydrogen bonds. For the mixed complexes, the C-Pots improve the BEs over those obtained without C-Pots from AD = 22.6% to AD = 8.5%. The C-Pots give the best improvement in AD for the dispersion-bound complexes, viz., 16.2% compared to ca. 68% obtained without C-Pots. In fact, two of the four stacked complexes, the uracil dimer and the indole−benzene dimers, are not stable without the use of C-Pots. The values we obtain for the hydrogen-bonded and mixed complexes are comparable to those obtained using the dispersion-corrected BLYP/TZV(2df,2pd) BEs reported by Grimme,[41] to the M06-2X/MG3S results of Zhang and Truhlar[40b] (see Table S4 in the SI), and to the ω-B97/6-311++G(3df,3pd) data reported by Chai and Head-Gordon.[14b] Note that the methods applied by

TABLE 5: Performance of PBE1/6-31+G(d,p) with Optimized Carbon Potentials in Comparison to B3LYP and B2-PLYP-D: Reaction Energies (kcal/mol) for a Series of Hydrocarbon Reactions and Conformational Changes with Strong Intramolecular Dispersion Effects[44]

	reaction	reference data[a]	PBE1/6-31+G(d,p)−C-Pots	B2-PLYP-D[a]	B3LYP[b]
1	$2C_{14}H_{10} \rightarrow C_{28}H_{20}$	−9.0[c]	−10.1	−6.1	25.4
2	[2.2]paracyclophane + $H_2 \rightarrow$ 2*p*-xylene	−58.5	−65.4	−59.2	−76.7
3	*n*-octane → tetramethylbutane	1.9	1.1	−2.4	8.5
4	*n*-undecane → hexamethylpentane	9.4	12.3	6.1	26.9
5	$C_{14}H_{30}$ (linear) → $C_{14}H_{30}$ (folded)	2.2	0.4	2.6	7.5
6	$C_{22}H_{46}$ (linear) → $C_{22}H_{46}$ (folded)	−3.6	0.2	−3.4	18.0
7	$C_{30}H_{62}$ (linear) → $C_{30}H_{62}$ (folded)	−8.8	0.0	−8.2	22.9

[a] See Table 5 and references therein of ref 42. B2PLYP-D/TZV(2df,2pd) on B3LYP/TZV(2d,2p) geometries. [b] Uncorrected, single-point B3LYP/TZV(2df,2pd) on TZV(2d,2p) geometries. [c] Determined using the diffusion Monte Carlo method (−9 ± 3 kcal/mol); see ref 45.

TABLE 6: Binding Energies (kcal/mol) for Coronene Dimers

dimer	PBE1/6-31G(d,p)−C-Pots[a]	ref 40b[b]
S	15.54	12.64 (9.77)
PD-1	22.55	21.73 (18.55)
TS	21.61	20.92 (17.59)

[a] PBE1/6-31+G(d,p) with C-Pots. [b] M06-2X/MG3S//M06-2X/DIDZ, with counterpoise-corrected energies in parentheses.

these other groups usually involve the use of very large basis sets and counterpoise corrections, both of which substantially increase the times required for calculations in comparison to those required using our approach.

2.2.2. Application to a Series of Reactions. As a further check of our approach, we applied the C-Pot method to a series of hydrocarbon reactions and conformational changes. This set of reactions has been collated by Grimme and co-workers to act as a general test of DFT methods for nonpolar hydrocarbon reactions involving strong intramolecular dispersion without the complication of electrostatics or charge transfer.[42]

Table 4 details the reaction energies determined using PBE1/6-31+G(d,p) with optimized C-Pots for this set of reactions and compares these data to those reported by Schwabe and Grimme[42] using uncorrected B3LYP/TZV(2df,2pd)//TZV(2d,2p) and by the dispersion-corrected B2-PLYP-D/TZV(2df,2pd)//B3LYP/TZV(2d,2p).

Reaction 1, the dimerization of anthracene, has notable relevance to the field of molecular electronics.[43] It is equally relevant to the current context of van der Waals forces since it involves both intermolecular and intramolecular dispersion. The hydrogenation of [2.2]paracyclophane (reaction 2) involves a structure with interatomic distances below typical van der Waals radii for carbon. Reactions 3 and 4 are branching isomerizations of sterically hindered hydrocarbons—a type of reaction that common DFT functionals (i.e., those that are not corrected for dispersion) fail to predict correctly given the contributions made by medium- and long-range electronic correlation. Reactions 5−7 are the folding about the center of large, straight-chained organics. The deficiencies of common DFT functionals are neatly highlighted by the reaction energies determined by B3LYP in Table 5.

In reaction 1, the failure of common DFT functionals to replicate the high-level (but not experimental)[45] reaction energy is a direct consequence of their inability to deal with strong intramolecular van der Waals interactions. For this reaction, our method gets to within 1.1 kcal/mol of the high-level value, an improvement on B2-PLYP-D/TZV(2df,2pd)//B3LYP/TZV(2d,2p) that is only within 2.9 kcal/mol. In fact, our method gives excellent agreement to high-level data for reactions 1−4. We are able to successfully predict the correct thermicity for reaction 3 (the branching of *n*-octane), in contrast to B2-PLYP-D/TZV(2df,2pd)//B3LYP/TZV(2d,2p), which fails in this regard. However, B2-PLYP-D/TZV(2df,2pd)//B3LYP/TZV(2d,2p) is more adept at prediction of conformational changes for large alkanes such as $C_{14}H_{30}$, $C_{22}H_{46}$, and $C_{30}H_{62}$ (reactions 5−7). This deficiency in our results is probably due to the error in the methane dimer interaction energy obtained with PBE1/6-31G(d,p)−C-Pots; see Table 2.

3. Application to Large, Polyaromatic Systems

We envisage this method to be particularly useful for large molecules. In such an instance it is undesirable to have to compute energies using large basis sets or to complete basis set limits or to have to use corrections for BSSE—all of which are time-consuming to the point of questioning the value of such a study. Up to this point, comparisons have been made between PBE1/6-31+G(d,p) with C-Pots and various DFT functionals that were designed with dispersion in mind. However, it is important to note that such comparisons are being made to data obtained with, generally, very large basis sets and often with the need for counterpoise corrections. PBE1/6-31+G(d,p) with C-Pots uses a relatively small basis set and does not require corrections for BSSE to predict comparable binding energies. Other B86-based functionals, e.g., B971 and PBE, will have similar performances.

We have applied PBE1/6-31+G(d,p) with optimized C-Pots, as outlined in the previous sections, to three sets of large molecules. Two of them are coronene and HBC since they are common prototypes for graphene.[40b] HBC[46] is also a common building block for synthesizable polynuclear hydrocarbon models of asphaltenes.[47,48] Coronene and HBC dimers contain substantial $\pi-\pi$ interactions. The third species in this series is an alkyl-substituted hexabenzocoronene, which contains alkyl−alkyl and $\pi-\pi$ stacking interactions to mimic the self-association properties of asphaltene fractions. As a starting point to our own understanding of the aggregation process, we have studied various configurations of HBC dimers and alkyl-substituted HBC dimers.

3.1. Coronene Dimer. We have studied three dimers of coronene—a sandwich, or parallel dimer (S), a parallel displaced structure (PD-1), and a twisted sandwich structure (TS) that possesses D_{6d} symmetry. In Table 6, we compare the binding energies determined in this work to those obtained using M06-2X/MG3S//DIDZ as detailed in ref 40b.

From Table 6 it is clear that the use of C-Pots with PBE1/6-31+G(d,p) gives binding energies comparable to those of M06-2X determined using a large basis set. This is especially true for the PD-1 and TS structures, with slightly greater discrepancy occurring for the S configuration. The discrepancies between our calculated data and those of Zhao and Truhlar

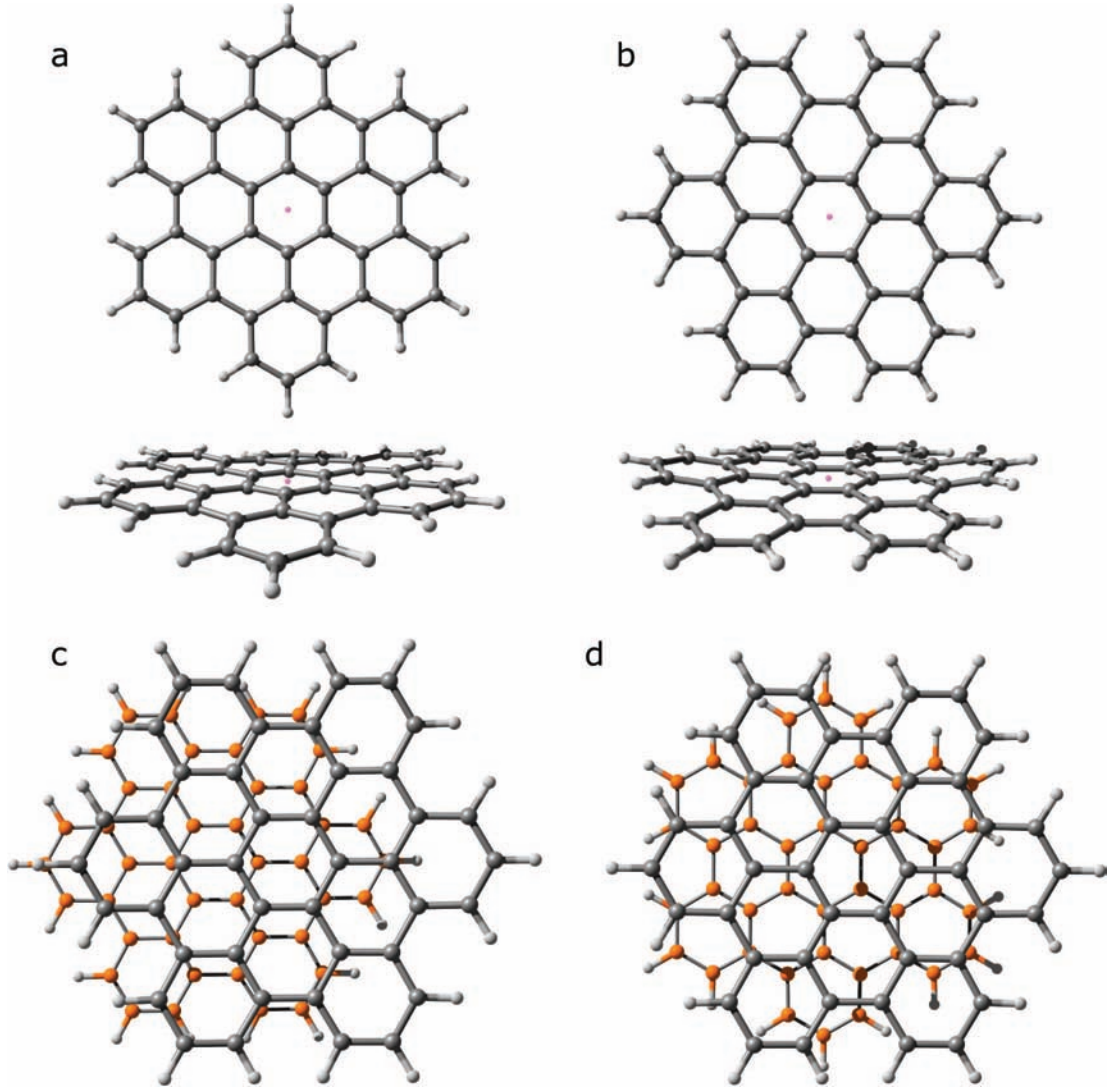

Figure 1. Perspective views of (a) a T-shaped hexabenzocoronene (HBC) dimer with the H atom of one monomer pointing toward the center of the π-system of the second monomer (BE = 5.2 kcal/mol, distance between approximate centers (indicated by purple spheres) 9.1 Å), a (b) T-shaped HBC dimer with four H atoms of one monomer pointed toward the center of the π-system of the second monomer (BE = 8.3 kcal/mol, distance between approximate centers 8.6 Å), (c) the C_{2h}-symmetric stacked HBC dimer (lowest energy structure) (BE = 44.8 kcal/mol, ring separation ~3.3 Å), and (d) the C_s-symmetric stacked HBC dimer. (BE = 43.5 kcal/mol, ring separation ~3.3 Å). For clarity in (c) and (d), the C atoms of the far HBC monomer are colored orange.

increase when the latter data are corrected for BSSE. We note that Grimme found a value of 21.6 kcal/mol for the PD-1 structure using DFT-D-BLYP/QZV(2df,2pd)//DFT-D-BLYP/TZV(2d,2p),[9a] which is closer to our calculated value and Zhao and Truhlar's non-counterpoise-corrected value.

Zhao and Truhlar[40b] find the vertical separation distance between planes to be 3.32 Å for PD-1 using M06-2X/DIDZ, while Ruusku and Pakkanen[49] report 3.41 Å (MP2/6-31G*), with a value of 3.40 Å determined by Grimme[9a] using BLYP-D/TZV(2d,2p) without counterpoise correction. PBE1/6-31+G(d,p) with C-Pots gives a separation of ca. 3.26 Å between planes. In the TS configuration we find a separation distance of 3.33 Å, which compares to 3.41 Å by M06-2X/DIDZ.

The binding data given in Table 6 indicate that the interaction in the π-stacked coronene dimers is strong enough to cause substantial electronic coupling between the fragments. The gap between the highest occupied molecular orbital (HOMO) and the lowest unoccupied molecular orbital (LUMO) in this dimer system is calculated to be 84.2 kcal/mol (3.65 eV).[50] This large gap implies that the coronene dimer is likely to be a poor model for bilayer graphene.[5]

3.2. Hexabenzocoronene. Numerous stable dimers exist in which one monomer lies perpendicular to the other. As might be expected, these are weakly bound species with typical binding energies of <10 kcal/mol. However, it is worthwhile to point out that such interactions are important in solid-state structures. Our calculations show that, in an orientation where only one H of a monomer is pointed toward the central part of the π-system of the other monomer (Figure 1a), the binding is 5.2 kcal/mol as compared to 8.3 kcal/mol when four H atoms are interacting (Figure 1b). There is also little difference in binding (ca. 1 kcal/mol) for configurations in which the H atoms of one monomer are pointing toward the edge of the π-system of the other monomer. The monomers to which the H atoms are pointing in these "T"-shaped structures display substantial distortions from planarity due to the interactions with the π-systems; see Figure 1a,b.

Greater binding is observed for those dimers exhibiting face-to-face interactions. Four HBC dimers with face-to-face interactions have been geometry optimized. They can be described as containing (1) C_{2h} symmetry (Figure 1c) and (2) C_s symmetry whereby the rings are displaced from each other along the

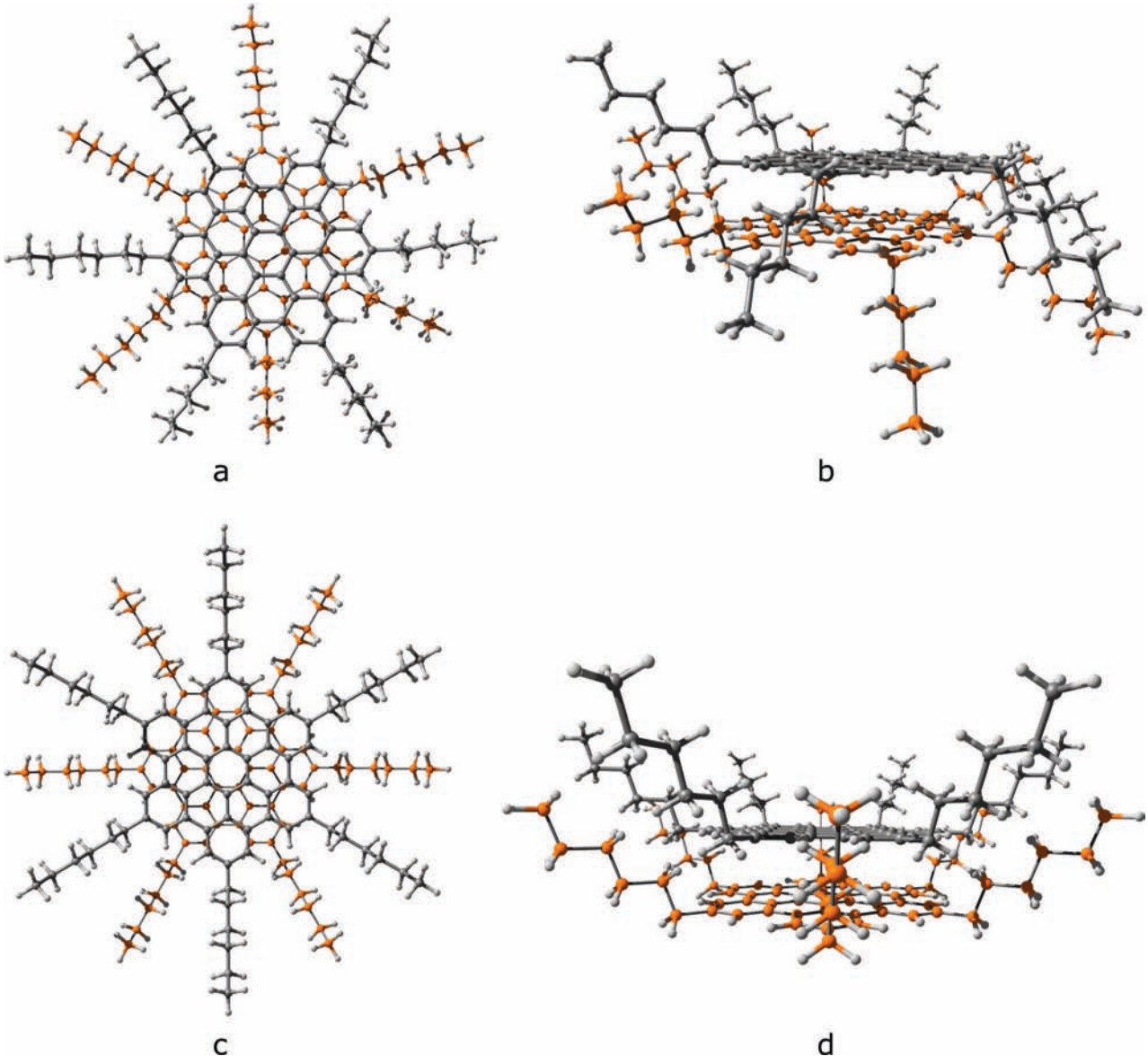

Figure 2. Perspective views of $(H_3C(CH_2)_5)_6$-HBC derivatives. C_s-symmetric structure: (a) top-down view and (b) side view (BE = 52.4 kcal/mol, ring separation ~3.4 Å). C_{6v}-symmetric structure: (c) top-down view and (d) side view (BE = 43.5 kcal/mol, ring separation ~3.3 Å).

direction perpendicular to the displacement witnessed in (1) (see Figure 1d) and as a (3) sandwich structure with D_{6d} symmetry and (4) D_{6h} sandwich that can be related to the parallel (S) structure of coronene.[51]

The lowest energy configuration has C_{2h} symmetry, which is similar to that seen in the crystal phase experimentally, but with less pronounced parallel displacement.[46] In this gas-phase study, the C_{2h} symmetrical structure is 1.3 kcal/mol more stable than, but with approximately the same center-of-mass distance, the C_s dimer (viz., BE = 43.5 kcal/mol, $r \approx 3.3$ Å). However, there is a marginal difference in energy between these and the BE of the D_{6d} structure, which are all within 3.1 kcal/mol. The D_{6h} isomer is less stable, being ca. 14 kcal/mol higher in energy than the C_{2h} structure. This is expected on the basis of the BE differences in the P-benzene/SP-benzene (see Table 2) and the S-coronene/PD-1-coronene (see Table 6) pairs.

HBC crystallizes into a monoclinic space group ($P2_1/a$), with a Y-packing arrangement, characterized by edge-to-face and offset face-to-face stacking between neighboring moieties.[46] This Y-packing is described in ref 46 as that in which the main C···C interactions are between parallel translated molecules, and this strength of interaction is borne out in our gas-phase calculations.

The HBC dimer with C_{2h} symmetry displays strong coupling similar to that found in the coronene PD-1 dimer, and the HOMO−LUMO gap in this system is 77.6 kcal/mol (3.37 eV).[50] The small difference in the HOMO energy shift and the HOMO−LUMO gap between the coronene and HBC dimers is typical of the slow approach to the asymptotic limit of the orbital shift as a function of the monomer/dimer size.

A "twisted" HBC trimer with D_{6h} symmetry has a calculated binding energy of 81.81 kcal/mol. In this system, each dimer subunit has approximate D_{6d} symmetry and the binding is essentially twice that of the aforementioned D_{6d} dimer to within 2%, thus suggesting an additive effect to the binding energy for such a system. This finding is consistent with those of Tauer and Sherrill[52] (and our subsequent efforts)[15] on benzene trimers which showed that there is no substantial cooperative effect in the binding of planar aromatics.

3.3. Hexasubstituted Hexabenzocoronene. Asphaltene model alkyl-HBC derivatives, such as the synthesized $(H_3C(CH_2)_{11})_6$-HBC, $(H_3C(CH_2)_8)_6$-HBC, and $(H_3C(CH_2)_5)_6$-HBC, have been shown experimentally to strongly self-associate in solution.[47,48,53] Experimental evidence, as measured by vapor-pressure osmometry, strongly suggests the formation of dimers[48] and other

oligomers in various solvents.[47] To explore dimer formation, we have optimized the geometries of two distinct dimer species for the $(H_3C(CH_2)_5)_6$-HBC derivative (hereafter C_6-HBC). These structures, which contain 336 atoms, are shown in Figure 2.

Parts a and b of Figure 2 show a structure with C_s symmetry, in which some of the C_6 alkyl chains are directed upward and some are directed downward relative to the planes defined by the aromatic moieties. The distance between the ring planes is ca. 3.4 Å in this optimized structure. Alternatively, the system can adopt a bowl-like configuration with C_{6v} symmetry, Figure 2c,d, with a separation between π-regions of ca. 3.3 Å. In this case, all alkyl chains are pointed in the same direction. The binding in both configurations is strong, with values of 52.4 and 43.5 kcal/mol for the C_s- and C_{6v}-symmetric structures, respectively. The difference of 8.9 kcal/mol suggests a preference for this dimer to adopt the former configuration. This can be partially explained by the inability of the C_{6v} structure to displace into a preferred slipped-parallel configuration. The differences in binding energy relative to the unsubstituted HBC structures are due to the interactions of the alkyl substituents. Our calculations therefore indicate that the lower binding energy of the C_s structure is the result of both enhanced $\pi-\pi$-interactions and alkyl−alkyl interactions. Our results suggest that, in solution, the C_6-HBC derivative likely has a stronger tendency to form structures of lesser order, rather than a highly ordered, discotic liquid-crystal-type structure.

4. Conclusions

The interactions within large, polyaromatic hydrocarbon dimers has been studied using density functional theory with corrections for dispersion. The dispersion corrections were implemented using carbon atom effective core-type potentials. These potentials are easily used with common computational chemistry programs and do not require any alteration of software. They can be applied to both pure and hybrid density functionals and be used in a variety of applications, including transition-state optimizations and frequency calculations. They add minimal computing time to calculations, and there is no requirement for accounting for basis set incompleteness.

The carbon potentials were optimized for use with standard B971, PBE, PBE1, PW91, B3LYP, and BHandHLYP DFT functionals in conjunction with 6-31G(d,p), 6-31+G(d,p), 6-311+G(2d,2p), and aug-cc-pVTZ basis sets. It was shown that the use of the potentials resulted in a dramatic improvement in the treatment of noncovalently bound dimer species in which the principal interaction between the monomers ranges from dispersion to hydrogen bonding. For a test set of common dimers, binding energies are predicted to within ca. 15%, and monomer separations to within ca. 0.1 Å, of high-level wave function data. The improvement in binding energies is a factor of ca. 3 over those obtained without the potentials.

We applied PBE1/6-31+G(d,p) with optimized carbon potentials to three sets of large, polyaromatic molecules. These included coronene and hexabenzocoronene, which are common prototypes for graphene, and alkyl-substituted hexabenzocoronene, which is a building block for synthesizable polynuclear hydrocarbon models of asphaltenes. These species contain substantial $\pi-\pi$ and/or alkyl−alkyl interactions.

We find excellent agreement of binding energies and structures for coronene dimer structures when compared to the results of other density functional theory methods in which dispersion is taken into account. Dimers of hexabenzocoronene show substantial binding for face-to-face interacting monomers, with the greatest effect (44.8 kcal/mol) seen for a C_{2h}, or parallel-displaced, structure. A $(H_3C(CH_2)_5)_6$-HBC derivative, composed of 336 atoms, wherein each monomer is hexaalkyl-substituted, also shows favorability for a displaced structure compared to a bowl-like orientation, with a difference in energy of 8.9 kcal/mol between these isomers. The overall binding energy in the parallel-displaced $(H_3C(CH_2)_5)_6$-HBC derivative is calculated to be 52.4 kcal/mol.

This work demonstrates a relatively straightforward approach to correcting the deficiencies in the treatment of long-range interactions by density function theory. The use of optimized carbon potentials with standard density functional methods offers an effective way of treating large, noncovalently bonded systems.

Acknowledgment. We thank the Centre of Excellence for Integrated Nanotools (CEIN) and Academic Information and Communication Technologies (AICT) at the University of Alberta, WestGrid, and Professor Pierre Boulanger for access to computing resources. We also thank the Program for Energy Research and Development (PERD) for funding.

Supporting Information Available: Optimized coefficients and binding energies with full tables. This information is available free of charge via the Internet at http://pubs.acs.org.

References and Notes

(1) Li, D.; Kaner, R. B. *Science* **2008**, *320*, 1170–1171.

(2) Mattheus, C. C.; de Wijs, G. A.; de Groot, R. A; Palstra, T. T. M. *J. Am. Chem. Soc.* **2003**, *125*, 6323–6330.

(3) The structure of asphaltene components is unknown. Several models have been proposed, including ones containing large, polyaromatic structures such as hexabenzocoronene.[4]

(4) For example, see: Alvarez-Ramirez, F.; Ramirez-Jaramillo, E.; Y. Ruiz-Morales, Y. *Energy Fuels* **2006**, *20*, 195–204.

(5) Kuzmenko, A. B.; van Heumen, E.; Carbone, F.; van der Marel, D. *Phys. Rev. Lett.* **2008**, *100*, 117401.

(6) Johnson, E. R.; DiLabio, G. A. *Chem. Phys. Lett.* **2006**, *419*, 333–339.

(7) Sato, T.; Tsuneda, T.; Hirao, K. *J. Chem. Phys.* **2007**, *126*, 234114.

(8) (a) von Lilienfeld, O. A.; Tavernelli, I.; Rothlisberger, U. *Phys. Rev. Lett.* **2004**, *93*, 153004. (b) von Lilienfeld, O. A.; Tavernelli, I.; Rothlisberger, U. *Phys. Rev. B* **2005**, *71*, 195119. (c) Lin, I.-C.; Coutinho-Neto, M. D.; Felsenheimer, C.; von Lilienfeld, O. A.; Tavernelli, I.; Rothlisberger, U. *Phys. Rev. B* **2007**, *75*, 205131.

(9) (a) Grimme, S. *J. Comput. Chem.* **2004**, *25*, 1463–1473. (b) Grimme, S. *J. Comput. Chem.* **2006**, *27*, 1787–1799. (c) Antony, J.; Grimme, S. *Phys. Chem. Chem. Phys.* **2006**, *8*, 5287–5293.

(10) (a) Johnson, E. R.; Becke, A. D. *J. Chem. Phys.* **2005**, *123*, 024101. (b) Johnson, E. R.; Becke, A. D. *J. Chem. Phys.* **2006**, *124*, 174104. (c) Johnson, E. R.; Becke, A. D. *J. Chem. Phys.* **2007**, *127*, 124108. (d) Johnson, E. R.; Becke, A. D. *J. Chem. Phys.* **2007**, *127*, 154108. (e) Johnson, E. R.; Becke, A. D. *J. Chem. Phys.* **2008**, *128*, 124105.

(11) (a) Zhao, Y.; Truhlar, D. G. *Phys. Chem. Chem. Phys.* **2005**, *7*, 2701–2705. (b) Zhao, Y.; Schultz, N. E.; Truhlar, D. G. *J. Chem. Theory Comput.* **2006**, *2*, 364–382. (c) Zhao, Y.; Truhlar, D. G. *J. Phys. Chem. A* **2004**, *108*, 6908–6918. (d) Zhao, Y.; Truhlar, D. G. *J. Phys. Chem. A* **2005**, *109*, 5656–5657.

(12) Dion, M.; Rydberg, H.; Schröder, E.; Langreth, D. C.; Lundqvist, B. I. *Phys. Rev. Lett.* **2004**, *92*, 246401.

(13) (a) Iikura, H.; Tsuneda, T.; Yanai, T.; Hirao, K. *J. Chem. Phys.* **2001**, *115*, 3540–3544. (b) Kamiya, M.; Tsuneda, T.; Hirao, K. *J. Chem. Phys.* **2000**, *117*, 6010. (c) Sato, T.; Tsuneda, T.; Hirao, K. *J. Chem. Phys.* **2005**, *123*, 104307.

(14) (a) Benighaus, T.; DiStasio, R. A., Jr.; Lochan, R. C.; Chai, J.-D.; Head-Gordon, M. *J. Phys. Chem. A* **2008**, *112*, 2702–2712. (b) Chai, J.-D.; Head-Gordon, M. *J. Chem. Phys.* **2008**, *128*, 084106.

(15) DiLabio, G. A. *Chem. Phys. Lett.* **2008**, *455*, 348–353.

(16) DiLabio, G. A.; Hurley, M. M.; Christiansen, P. A. *J. Chem. Phys.* **2002**, *116*, 9578–9584.

(17) Moon, S.; Christiansen, P. A.; DiLabio, G. A. *J. Chem. Phys.* **2004**, *120*, 9080–9086.

(18) DiLabio, G. A.; Dogel, S. A.; Wolkow, R. A. *Surf. Sci.* **2006**, *600*, L209–L213.

(19) Frisch, M. J.; Trucks, G. W.; Schlegel, H. B.; Scuseria, G. E.; Robb, M. A.; Cheeseman, J. R.; Montgomery, J. A., Jr.; Vreven, T.; Kudin, K. N.;

Burant, J. C.; Millam, J. M.; Iyengar, S. S.; Tomasi, J.; Barone, V.; Mennucci, B.; Cossi, M.; Scalmani, G.; Rega, N.; Petersson, G. A.; Nakatsuji, H.; Hada, M.; Ehara, M.; Toyota, K.; Fukuda, R.; Hasegawa, J.; Ishida, M.; Nakajima, T.; Honda, Y.; Kitao, O.; Nakai, H.; Klene, M.; Li, X.; Knox, J. E.; Hratchian, H. P.; Cross, J. B.; Adamo, C.; Jaramillo, J.; Gomperts, R.; Stratmann, R. E.; Yazyev, O.; Austin, A. J.; Cammi, R.; Pomelli, C.; Ochterski, J. W.; Ayala, P. Y.; Morokuma, K.; Voth, G. A.; Salvador, P.; Dannenberg, J. J.; Zakrzewski, V. G.; Dapprich, S.; Daniels, A. D.; Strain, M. C.; Farkas, O.; Malick, D. K.; Rabuck, A. D.; Raghavachari, K.; Foresman, J. B.; Ortiz, J. V.; Cui, Q.; Baboul, A. G.; Clifford, S.; Cioslowski, J.; Stefanov, B. B.; Liu, G.; Liashenko, A.; Piskorz, P.; Komaromi, I.; Martin, R. L.; Fox, D. J.; Keith, T.; Al-Laham, M. A.; Peng, C. Y.; Nanayakkara, A.; Challacombe, M.; Gill, P. M. W.; Johnson, B.; Chen, W.; Wong, M. W.; Gonzalez, C.; Pople, J. A. *Gaussian 03*, revision D.01; Gaussian Inc.: Pittsburgh, PA, 2004.

(20) MOLPRO, version 2006.1, a package of ab initio programs: Werner, H.-J.; Knowles, P. J.; Lindh, R.; Manby, F. R.; Schütz, M.; Celani, P.; Korona, T.; Rauhut, G.; Amos, R. D.; Bernhardsson, A.; Berning, A.; Cooper, D. L.; Deegan, M. J. O.; Dobbyn, A. J.; Eckert, F.; Hampel C.; Hetzer, G.; Lloyd, A. W.; McNicholas, S. J.; Meyer W.; Mura, M. E.; Nicklass, A.; Palmieri, P.; Pitzer, R.; Schumann, U.; Stoll, H.; Stone, A. J.; Tarroni, R.; Thorsteinsson, T. See http://www.molpro.net.

(21) Perdew, J. P.; Burke, K.; Ernzerhof, M. *Phys. Rev. Lett.* **1996**, *77*, 3865–3868.

(22) Perdew, J. P.; Chevary, J. A.; Vosko, S. H.; Jackson, K. A.; Pederson, M. R.; Singh, D. J.; Fiolhais, C. *Phys. Rev. B* **1992**, *46*, 6671–6687.

(23) Hamprecht, F. A.; Cohen, A. J.; Tozer, D. J.; Handy, N. C. *J. Chem. Phys.* **1998**, *109*, 6264–6271.

(24) Adamo, C.; Barone, V. *J. Chem. Phys.* **1999**, *110*, 6158–6169.

(25) Becke, A. D. *J. Chem. Phys.* **1993**, *98*, 5648–5652.

(26) Lee, C.; Yang, W.; Parr, R. G. *Phys. Rev. B* **1988**, *37*, 785–789.

(27) As implemented in ref 19.

(28) Boys, S. F.; Bernardi, F. *Mol. Phys.* **1970**, *19*, 553–566.

(29) Tsuzuki, S.; Honda, K.; Uchimaru, T.; Mikami, M. *J. Chem. Phys.* **2004**, *120*, 647–659.

(30) Zhang, Y.; Pan, W.; Tang, W. *J. Chem. Phys.* **1997**, *107*, 7921–7925.

(31) Tsuzuki, S.; Honda, K.; Uchimaru, T.; Mikami, M.; Tanabe, K. *J. Am. Chem. Soc.* **2000**, *122*, 3746–3753.

(32) Zhao, Y.; Truhlar, D. G. *J. Chem. Theory Comput.* **2005**, *1*, 415–432.

(33) Sinnokrot, M. O.; Sherrill, C. D. *J. Phys. Chem. A* **2004**, *108*, 10200–10207.

(34) Tsuzuki, S.; Uchimaru, T.; Mikami, M.; Urata, S. *J. Chem. Phys.* **2002**, *116*, 3309–3315.

(35) Tsuzuki, S.; Uchimaru, T.; Mikami, M.; Tanabe, K. *J. Chem. Phys.* **1998**, *109*, 2169–2175.

(36) Tsuzuki, S.; Honda, K.; Uchimaru, T.; Mikami, M.; Tanabe, K. *J. Am. Chem. Soc.* **2000**, *122*, 11450–11458.

(37) Jurečka, P.; Šponer, J.; Černý, J.; Hobza, P. *Phys. Chem. Chem. Phys.* **2006**, *8*, 1985–1993.

(38) As an illustrative example, see: Grimme, S.; Steinmatz, M.; Korth, M. *J. Org. Chem.* **2007**, *72*, 2118–2126.

(39) The S22 set also contains dimers that do not have carbon atoms (e.g., water and ammonia dimer) and were excluded because binding energies in these systems do not provide a test of the C-Pot approach. For completeness, dimers containing exclusively non-carbon atoms are included in Table S4 in the SI.

(40) (a) Zhao, Y.; Truhlar, D. *Theor. Chem. Acc.* **2008**, *119*, 525−525; *120*, 215−241. (b) Zhao, Y.; Truhlar, D. *J. Phys. Chem. C* **2008**, *112*, 4061–4067.

(41) Grimme, S.; Antony, J.; Schwabe, T.; Mück-Lichtenfeld, C. *Org. Biomol. Chem* **2007**, *5*, 741–758.

(42) Schwabe, T.; Grimme, S. *Phys. Chem. Chem. Phys.* **2007**, *9*, 3397–3406.

(43) For a recent perspective, see: Malliaras, G.; Friend, R. *Phys. Today* **2005**, *58*, 53–58, and references therein.

(44) It should be noted that reactions 1 and 2 convolute strong dispersion effects with bond formation/scission processes, so these reactions cannot be used to neatly assess the ability of the applied methods to predict dispersion interactions. They are included here for completeness.

(45) Grimme, S.; Diedrich, C.; Korth, M. *Angew. Chem., Int. Ed.* **2006**, *45*, 625–629. This reference explains the discrepancy between experiment and theory behind the energetics of the dimerization of anthracene.

(46) Goddard, R.; Haenel, M. W.; Herndon, W. C.; Krüger, C.; Zander, M. *J. Am. Chem. Soc.* **1995**, *117*, 30–41.

(47) For a review, see: Watson, M. D.; Fechtenkötter, A.; Müllen, K. *Chem. Rev.* **2001**, *101*, 1267–1300.

(48) Rakotondradany, F.; Feniri, H.; Rahimi, P.; Gawrys, K. L.; Kilpatrick, P. K.; Gray, M. *Energy Fuels* **2006**, *20*, 2439–2447.

(49) Ruusku, H.; Pakkanen, T. A. *J. Phys. Chem. B* **2001**, *105*, 9541–9547.

(50) We recognize that calculated LUMO energies are not always reliable and care must be taken when drawing conclusions based on such data.

(51) It should be pointed out that the use of symmetry in the geometry optimizations of these dimers restricts the degrees of freedom of the monomers within the dimers during geometry optimizations.

(52) Tauer, T. P.; Sherrill, C. D. *J. Phys. Chem. A* **2005**, *109*, 10475–10478.

(53) Tchebotareva, N.; Yin, Y.; Watson, M. D.; Samori, P.; Rabe, J. P.; Müllen, K. *J. Am. Chem. Soc.* **2003**, *125*, 9734–9739.

JP806162T